Direct and indirect photoluminescence excitation and ultraviolet emission from Tm-doped $Al_xGa_{1-x}N$

Yuri D. Glinka,[1,2] John V. Foreman,[1,3] Henry O. Everitt,[1,3,a)] Don S. Lee,[4] and Andrew J. Steckl[4]
[1]*U.S. Army Aviation and Missile RDEC, Redstone Arsenal, Alabama 35898, USA*
[2]*Nano and Micro Devices Center, University of Alabama in Huntsville, Huntsville, Alabama 35899, USA*
[3]*Department of Physics, Duke University, Durham, North Carolina 27708, USA*
[4]*Nanoelectronics Laboratory, University of Cincinnati, Cincinnati, Ohio 45221, USA*

(Received 31 December 2008; accepted 10 February 2009; published online 17 April 2009)

We provide experimental evidence for direct and indirect excitations of photoluminescence (PL) from Tm-doped $Al_xGa_{1-x}N$ of varying Al content. Direct excitation of Tm^{3+} ions is observed primarily at 85 K through transitions $^3H_6 \rightarrow {}^1I_6$, $^3P_0$, $^3P_1$, and $^3P_2$ when these levels are below the absorption edge of the $Al_xGa_{1-x}N$ for a given Al content. Strong ultraviolet emission at 298 nm ($^1I_6 \rightarrow {}^3H_6$), 355 nm ($^1I_6 \rightarrow {}^3F_4$), and 371 nm ($^1D_2 \rightarrow {}^3H_6$), as well as the familiar blue emission at 463 nm ($^1D_2 \rightarrow {}^3F_4$), and 479 nm ($^1G_4 \rightarrow {}^3H_6$), is found to depend sensitively on the Al content, excitation wavelength (i.e., direct or indirect), excitation type (continuous wave versus pulsed), and upper state of the transition. PL excitation spectroscopy and time-integrated and time-resolved PL spectra are compared to elucidate the complex energy transfer pathways. © *2009 American Institute of Physics*. [DOI: 10.1063/1.3098256]

INTRODUCTION

Rare-earth (RE) ions incorporated into semiconductors present an interesting possibility for integrated light-emitting devices.[1] Despite the numerous known applications of RE-doped III-V semiconductors for linear and nonlinear optics and laser physics, a better understanding of energy transfer from the semiconductor host to the RE ions is still needed. The effective excitation cross section of RE ions is dramatically increased when carriers are "indirectly" photoexcited in wide bandgap semiconductor host materials: an Auger-type process efficiently transfers energy to the RE intra-4*f* electron levels from the nonradiative recombination of excitons trapped at RE-related sites.[2–5] These sites may be RE substitutions at group III sites or, as suggested by local density functional calculations, RE-vacancy defect complexes.[6–8] Subsequently, narrow, long-lived visible light emission is observed from lower 4*f* levels.

Lee and Steckl investigated Tm-doped $Al_xGa_{1-x}N$ alloys grown by molecular-beam epitaxy.[9] Their electroluminescence (EL) data indicated strong, narrow, blue emission at 463 nm ($^1D_2 \rightarrow {}^3F_4$) and 479 nm ($^1G_4 \rightarrow {}^3H_6$) whose relative strength varied with Al content (x). Using the same $Tm:Al_xGa_{1-x}N$ samples, Hömmerich *et al.* studied the strength and decay of these and other lines using photoluminescence (PL) spectroscopy, observing somewhat different variations with x and a sensitivity to excitation wavelength.[4] To explore these dependences, we present our investigation of these samples using continuous wave (cw) and pulsed time-integrated and time-resolved PL and cw PL excitation (PLE) spectroscopy, emphasizing these two blue transitions plus three surprisingly strong ultraviolet transitions at 298 nm ($^1I_6 \rightarrow {}^3H_6$), 355 nm ($^1I_6 \rightarrow {}^3F_4$), and 371 nm ($^1D_2 \rightarrow {}^3H_6$).

Specifically, we observe experimentally both direct and indirect excitations of Tm^{3+}-related PL and analyze the complex manner in which the PL and PLE spectra vary with x as the bandgap energy of $Al_xGa_{1-x}N$ moves relative to the Tm^{3+} energy levels. Here, direct excitation of Tm^{3+} occurs if the pump wavelength is coincident with transition energies from the $^3H_6$ ground state to excited states $^1I_6$, $^3P_0$, $^3P_1$, and $^3P_2$ when the latter is below the conduction band of $Al_xGa_{1-x}N$ for a given x. By contrast, the indirect mechanism occurs when the excitation wavelength is above the bandgap of the host, and energy transfer occurs through the Auger process mentioned above. In order to reconcile differences among the various reports on $Tm:Al_xGa_{1-x}N$ emission, the strength and decay at least 14 4*f* transitions were studied as a function of x, excitation wavelength (i.e., direct or indirect), excitation type (i.e., cw or pulsed), and upper state ($^1I_6$, $^1D_2$, and $^1G_4$).

Tm-doped $Al_xGa_{1-x}N$ materials of $x=0.39$, 0.62, 0.81, and 1.0 used in the current study were grown by solid-source molecular-beam epitaxy on *p*-type Si (111) substrates. The growth procedure has been previously discussed.[9] The tunable cw light source for PLE spectroscopy was a xenon arc lamp dispersed through an Acton 150 mm monochromator. For time-integrated and time-resolved PL measurements, a Quantronix TOPAS optical parametric amplifier (OPA), which was pumped by a 1 kHz regenerative amplifier seeded by a 80 MHz Ti:sapphire oscillator ($\lambda=790$ nm), has been used as a pulsed source. In our experiments, the OPA was tuned to 238, 261, and 323 nm (5.21, 4.75, and 3.84 eV), with an average intensity of 20 mW and pulse width of ~200 fs, to excite PL. Throughout the text when pulsed excitation data is presented, the wavelength used is 238 nm

a)Author to whom correspondence should be addressed. Electronic mail: henry.o.everitt@us.army.mil.

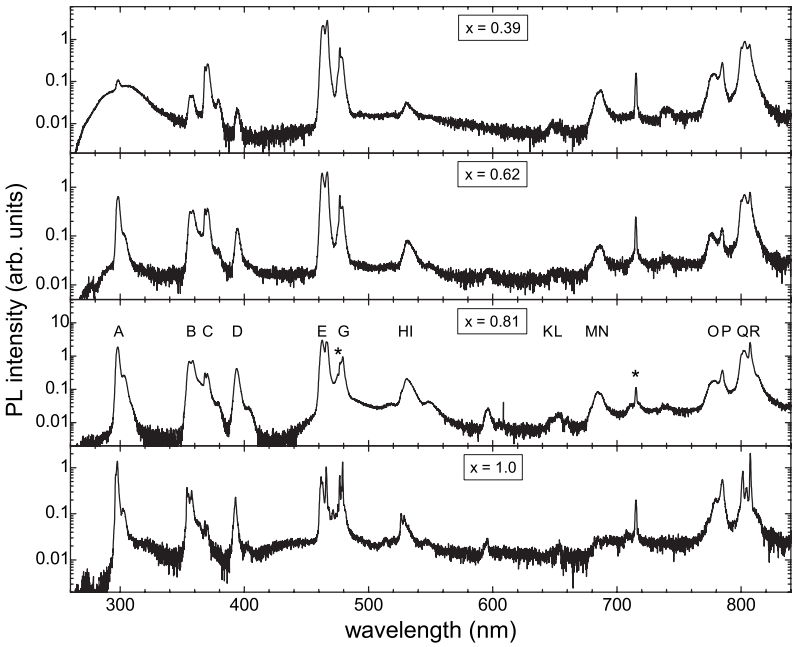

FIG. 1. PL spectra for Tm^{3+}:$Al_xGa_{1-x}N$ of different x measured with 5.21 eV pulsed excitation at 85 K. A logarithmic scale was used to allow the evolution of weak features to be seen more clearly. Transitions are labeled by letters referenced to Fig. 2. The narrow, starred features at 476 and 714 nm are the second and third order diffractions of the laser light, respectively.

unless otherwise specified. The time-integrated PL was dispersed by a 0.30 m imaging spectrometer and measured using a liquid nitrogen-cooled charge-coupled device camera. For cw PL and PLE, the detection system was a 0.75 monochromator (SPEX) with photomultiplier tube (Hamamatsu R928) using standard lock-in detection techniques. A streak camera monitored the time-resolved PL response with temporal resolution chosen between 10 and 100 ns for most measurements.

SPECTROSCOPY

Figure 1 shows the time-integrated pulsed PL spectra for Tm-doped $Al_xGa_{1-x}N$ of different x measured at 85 K. The spectra reveal several sharp features that are attributed to $4f$ transitions in Tm^{3+} ions.[4,9,10] The 14 observed $4f$ transitions and corresponding energy level diagram for each x are indicated in Fig. 2, including the familiar blue emission features

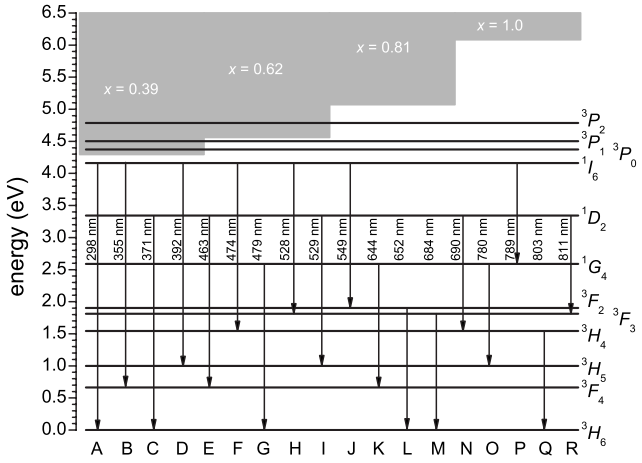

FIG. 2. Energy diagram for Tm^{3+}:$Al_xGa_{1-x}N$, labeling each of the observed PL and PLE transitions. The conduction band states for the $Al_xGa_{1-x}N$ materials of different x are shown in gray. The wavelengths used typically represent the strongest feature of the multiplet and correspond to a self-consistent assignment of the energy of the levels.

and other UV and visible transitions starting from the $^1I_6$, $^1D_2$, $^1G_4$, and $^3H_4$ multiplet manifolds. Within the experimental uncertainty of ± 1 meV, the wavelengths of these transitions were unaffected by changes in x and temperature (up to 300 K).

Many transitions appear as broad (4–5 nm wide) singlets, most prominently $^1G_4 \rightarrow {}^3H_6$, while others appear as doublets, such as $^1D_2 \rightarrow {}^3F_4$. The broad linewidths imply underlying unresolved fine structure due to crystal field splitting.[10] For example, these two blue transitions evolve with increasing x from broad (4–5 nm) singlets and doublets to numerous spectrally resolved narrow (<1 nm) fine structure lines, especially for $x=1.0$ where at least 11 interleaved components are resolved at 85 K. Many transitions, particularly those involving $^1D_2$ and $^3F_4$ ($^1I_6 \rightarrow {}^3F_4$, $^1D_2 \rightarrow {}^3F_4$, $^1G_4 \rightarrow {}^3F_4$, and $^1D_2 \rightarrow {}^3H_6$), appear as broad doublets with an $\sim$20 meV separation that widens with increasing x until the fine structure is fully resolved at $x=1.0$. For example, the splitting of the $^1I_6 \rightarrow {}^3F_4$ (355 nm) and $^1D_2 \rightarrow {}^3H_6$ (371 nm) doublets slightly widens with increasing x until at least six fine structure components are resolved for $x=1.0$. This evolution suggests that the Tm^{3+} ions experience at least two local environments within $Al_xGa_{1-x}N$ hosts, perhaps substitution at both Al and Ga sites, whose corresponding fine structure overlaps to form the observed broad feature that increasingly resolves as Al replaces Ga with increasing x.

The most intense PL peaks have been used as the registration wavelength (λ_{reg}) for measuring the corresponding cw PLE spectra (Fig. 3). For all samples, the PLE rises strongly with the absorption edge of the $Al_xGa_{1-x}N$ host, which was measured to shift to higher energy with increasing x: 4.28 eV ($x=0.39$), 4.55 eV ($x=0.62$), and 5.06 eV ($x=0.81$).[11] This confirms that the PL from Tm^{3+} is most efficiently excited indirectly. (Indeed, emission from the $x=1.0$ sample is weak because only direct excitation of the Tm^{3+} is possible with our apparatus.) High energy "absorbing" levels (i.e., $^1I_6$, $^3P_0$, $^3P_1$, and $^3P_2$) are the conduit for indirect transfer to Tm^{3+},

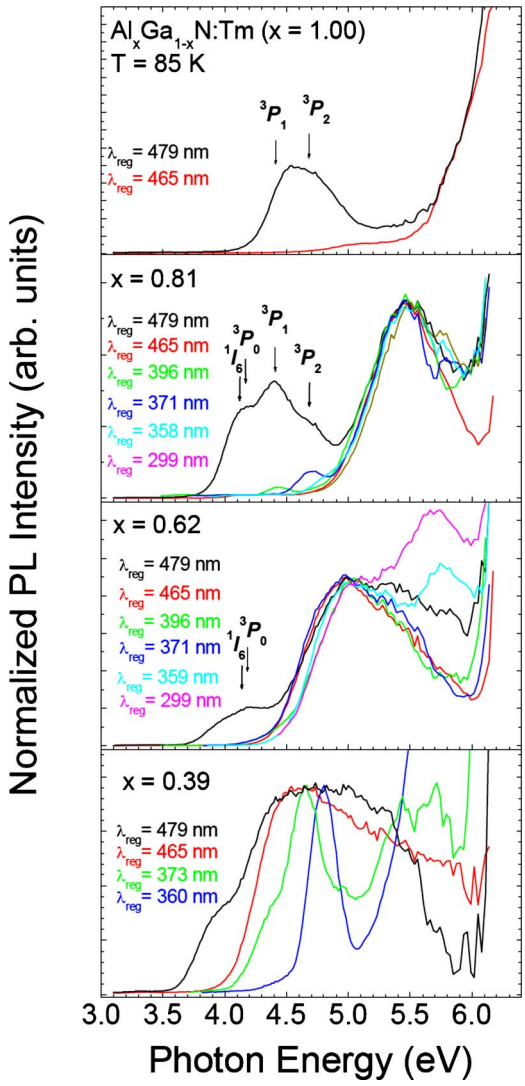

FIG. 3. (Color online) PLE spectra at 85 K for Tm^{3+}:$Al_xGa_{1-x}N$ of different x. Spectra measured at different λ_{reg} are shown by the corresponding colors. The labels indicate the wavelength of the multiplet component measured, which is not always the primary component specified in Fig. 2. The $^1I_6$ and ^3P_J levels of Tm^{3+} are indicated by arrows.

but no emission is observed from any of the ^3P_J levels. Instead, most observed PL transitions start from the $^1I_6$, $^1D_2$, or $^1G_4$ levels. Energy transfer—from photogenerated excitons in the host, to trapped excitons at the dopant site, to excitation of the absorbing Tm^{3+} levels via the Auger process, to relaxation to the emitting levels—occurs rapidly and nonradiatively compared to the slow, radiative decay from the emitting levels, as will be discussed below.

Considering first the cw source used for PLE, every transition for which PL is observed could be excited indirectly. However, only the $^1G_4 \rightarrow {}^3H_6$ transition (479 nm) could be excited directly, through the absorbing transitions $^3H_6 \rightarrow {}^1I_6$, $^3P_0$, $^3P_1$, and $^3P_2$. The arrows shown in Fig. 3 correspond to the peak absorption energies for these transitions in $Tm:Al_xGa_{1-x}N$, whose values are near those found by Gruber *et al.* for Tm:AlN.[10] Direct excitation is observed for $x=0.62$, 0.81, and 1.0, but not for $x=0.39$ since the bandgap is below those absorbing states. It is noteworthy that the UV and blue emitting transitions from $^1I_6$ (298, 355, and 392 nm) and $^1D_2$ (371 and 463 nm) were not observable using cw direct excitation.[12]

Returning to pulsed excitation, for a given sample (fixed x) all lines strengthen as the excitation wavelength decreases, most dramatically when excitation changes from direct to indirect. The PL intensity is largest when the excitation energy is just above the $Al_xGa_{1-x}N$ bandgap, an indication of efficient trapping and energy transfer from excitons to Tm^{3+} ions. While PL from only one transition is observed for cw direct excitation, PL is observed from all transitions for pulsed direct excitation. Moreover, the strength of each PL feature depends on x, the upper state of the emission, and whether excitation is direct or indirect.

(1) The observed PL strength from the strongest $^1G_4$ transition ($^1G_4 \rightarrow {}^3H_6$ at 479 nm) is remarkably insensitive to x and excitation wavelength, whether pumped indirectly or directly.

(2) Even though the blue $^1D_2 \rightarrow {}^3F_4$ transition (463 nm) almost completely disappears for direct, cw excitation (Fig. 3), it exhibits the strongest PL of all transitions under direct, pulsed excitation for $x=0.39$ and 0.61. Indeed, all five observed $^1D_2$ transitions ($\rightarrow {}^3F_2, \rightarrow {}^3H_4, \rightarrow {}^3H_5, \rightarrow {}^3F_4, \rightarrow {}^3H_6$) are strong under direct excitation ($\lambda=323$ nm), but they weaken with increasing x. For example, the $^1D_2 \rightarrow {}^3F_4$ transition weakens under direct pulsed excitation relative to the $^1G_4 \rightarrow {}^3H_6$ transition with increasing x from ~3:1 ($x=0.39$) to ~1:1 ($x=1.0$). However, when pumped indirectly, Fig. 1 reveals that the relative strengths of these two transitions remains fairly insensitive to x, maintaining a strength ratio of ~5:1 just as was seen for above bandgap, indirect cw excitation.

(3) In contrast with the $^1D_2$ transitions, the five transitions observed from the $^1I_6$ state ($\rightarrow {}^1G_4, \rightarrow {}^3F_2, \rightarrow {}^3H_5, \rightarrow {}^3F_4, \rightarrow {}^3H_6$) grow stronger as x increases, particularly for indirect excitation (Fig. 1). Indeed, the $^1I_6$ transitions are quite sensitive to x, barely observable for the $x=0.39$ (indirect excitation) sample but are among the strongest PL features for the $x=0.81$ (indirect) and 1.0 (direct) samples, especially $^1I_6 \rightarrow {}^3H_6$ (298 nm). The pair of UV transitions $^1I_6 \rightarrow {}^3F_4$ (355 nm) and $^1D_2 \rightarrow {}^3H_6$ (371 nm) dramatically reveals how $^1I_6$ and $^1D_2$ have different sensitivities to x: the strength ratio changes as ~1:6, 1:1, ~3:1, and ~6:1 for $x=0.39$, 0.62, 0.81 (all indirect) and 1.0 (direct), respectively.

Thus, PL from $^1I_6$ transitions grows stronger with x, while PL from $^1D_2$ transitions weakens with x for pulsed excitation, suggesting a competition between the energy transfer pathways that supply these levels.

ENERGY TRANSFER

How can these observations be explained? Regarding excitation, indirect excitation is much more efficient than direct, especially for cw. Short wavelength excitation is more efficient than long for all samples regardless of whether the excitation is direct or indirect. In addition to transfer from

the host to the absorbing levels $^1I_6$, $^3P_0$, $^3P_1$, and $^3P_2$ through the Auger process, cw PLE and especially pulsed excitation PL indicate direct absorption into the absorbing levels occurs for samples whose bandgap is above them. These three observations confirm that these high lying absorbing levels are involved in the energy transfer pathways that excite the "emitting" transitions from $^1I_6$, $^1D_2$, and $^1G_4$.

However, why is emission only observed from the $^1G_4$ transition for cw direct excitation, while emission is observed from all $^1I_6$, $^1D_2$, and $^1G_4$ transitions for pulsed direct excitation at the same below bandgap wavelength? An important clue comes from Hömmerich *et al.*, who, using a tunable OPO with 10 ns wide pulses, observed the $^1D_2$ transitions in Tm:AlN only when excited above 4.4 eV.[4] This is just above the energy of the $^3P_0$ energy (4.37 eV) estimated by Gruber *et al.*[10] Hömmerich *et al.* also observed that the $^1G_4$ transition continues to be strong until the excitation drops below 4.13 eV, which is near the energy of the $^1I_6$ level (4.18 eV). This suggests favored energy transfer pathways within Tm^{3+}; namely, $^3P_0 \rightarrow {}^1D_2$ and $^1I_6 \rightarrow {}^1G_4$. Although the former transition ($\lambda \approx 1230$ nm) was not observable with our spectrometer, the $^1I_6 \rightarrow {}^1G_4$ transition is observed at 789 nm among the many spectral components near 800 nm, including $^1D_2 \rightarrow {}^3F_3$, $^1G_4 \rightarrow {}^3H_5$, and $^3H_4 \rightarrow {}^3H_6$.

Supposing then that $^1D_2$ receives its excitation preferentially from $^3P_0$ while $^1G_4$ is strongest when it receives its excitation via $^1I_6$, it further appears that some sort of competition for excitation occurs between $^1I_6$, $^1D_2$, and $^1G_4$. Because many features of the 10 ns pulsed PL of Hömmerich *et al.* are similar to our cw PL but different from our 200 fs pulsed PL, it appears that this competition for excitation between $^1I_6$, $^1D_2$, and $^1G_4$ is resolved by a critical quasiequilibrium that is established on a time scale between 200 fs and 10 ns. Exciton cooling, exciton trapping, and Auger transfer happen very quickly (picosecond time scales), so it is likely that the rate-limiting step for this equilibration involves the (nonradiative) redistribution of excitation among the absorbing levels $^1I_6$, $^3P_0$, $^3P_1$, and $^3P_2$. Indeed, this appears to depend on which levels are directly excited by the laser and the quantum mechanical transition matrix element "branching ratios" that connect the absorbing and emitting levels $^1I_6$, $^1D_2$, and $^1G_4$. This, in turn, is mediated by the changing lattice morphology as the host evolves from GaN-like to AlN-like and more of the Tm^{3+} substitutes for Al instead of Ga. Because it is observed experimentally that $^1D_2$ suffers as a result of this equilibration relative to $^1I_6$ and $^1G_4$, it would appear that $^3P_0$ is not favored in this equilibration and that $^1I_6$ and $^1D_2$ are not well connected. However, if $^3P_0$ is excited fast enough (i.e., directly with a 200 fs pulse or indirectly in picoseconds), $^1D_2$ fares better and emits much more strongly.

To explore this redistribution, the temporal evolution of $Al_xGa_{1-x}N$ and Tm^{3+} -related PL has been measured at 85 K for the most intense features. First, notice the broadband feature centered at 295 nm, which was observed for $x=0.39$ and 0.62 (Fig. 1). This is the shallow impurity band PL through which the Auger-type mechanism of indirect PLE occurs.[13] Time-resolved measurements confirm earlier findings that this feature decays quickly, faster than the temporal resolution of the streak camera (30 ps).[14] Next, regarding the Tm^{3+} lines themselves, the rise times were very fast compared to the slow decay times (0.5–15 μs). Thus, all the processes of energy transfer between the hosts and Tm^{3+} ions occur in a time frame that is much shorter than the lifetime of light emitters.

The single exponential decay time constants depend on the upper level of the emitting transition but are surprisingly insensitive to lower level, Al content, and excitation wavelength, including direct and indirect excitations. The measured decay constants in (μs) are $^1I_6$: 0.5 (1), 1.3 (2); $^1D_2$: 1.2 (2), 1.4 (3); $^1G_4$: 6.6 (4), 15.0 (5) for 300 and 85 K, respectively, where the numbers in parentheses represent the uncertainty in the least significant digit. These values are slightly faster and more temperature sensitive than the values reported previously, but they confirm the earlier conclusion that nonradiative relaxation minimally competes with radiative decay.[4]

Now, recall that a connection between $^1I_6$ and $^1G_4$ was established above but that emission from $^1I_6$ to at least four other levels was also measured. This means that slowly decaying $^1G_4$ must compete for excitation, via branching ratios, with these other levels during the short period of time $^1I_6$ is populated. This explains why cw direct excitation of $^1G_4$ is observed; namely, that cw excitation keeps the $^1I_6$ level populated so it, in turn, can keep $^1G_4$ populated. The branching ratios clearly favor the strong Tm^{3+} $^1I_6$ UV lines at 298 and 355 nm and suggest that they increasingly prefer these transitions with increasing x. Likewise, the branching ratios from the ^3P_J levels change with increasing x to favor processes that excite $^1I_6$ (and $^1G_4$) over those that excite $^1D_2$. This may be exploited to devise optically or electrically excited bright, narrowband UV emitters for spectroscopic and active sensing applications.

In light of this analysis, let us compare the three reports describing the relative strength of the blue features (463 nm:479 nm) as a function of x (0.39, 0.62, 0.81, and 1.0). In the first report, 120 V cw EL spectra showed the 463 nm feature grew rapidly from much weaker to much stronger (0.3:1, unknown, 1.2:1 and 3:1).[9] In the second, 10 ns pulsed excitation at $\lambda=250$ nm showed that the 463 nm feature is always much stronger (3:1, ~10:1, ~10:1, and 5:1), where the first two represent indirect excitation and the last two represent direct excitation.[4] In our report, when exciting the sample above the bangap, the 463 nm feature was approximately five times stronger for all x regardless of whether the excitation was cw or pulsed. However, when excited directly using the 323 nm, 200 fs pump, the 463 feature weakens with x (3:1, 3.5:1, 2:1, and 1:1). What clearly emerges is that the emission behavior sensitively depends on excitation conditions. The evolution of PL with x is explained by evolving local environments at the dopant sites that alter the branching ratios of the internal relaxation pathways. Which pathways are active and to what extent they participate depend sensitively on the excitation wavelength (i.e., where the excitons start) and duration (i.e., how much equilibration occurs among the pathways). In extreme regimes, additional processes may also contribute,

such as hot electron impact ionization for the EL data. It is therefore important to choose appropriate excitation conditions when developing Tm:AlGaN-based devices.

SUMMARY

In summary, we have observed both direct and indirect excitations of PL from Tm-doped $Al_xGa_{1-x}N$ materials of different Al contents. The direct excitation regime is observed when the Tm^{3+} absorptive transitions do not overlap with the band-to-band transitions in the $Al_xGa_{1-x}N$ host. The sensitive dependence of the emission properties on x, excitation wavelength, excitation conditions (cw versus pulsed), and upper state of the emitter were explored using various cw, time-integrated, and time-resolved spectroscopies. An explanation for the excitation dependence of the two blue emission lines is offered, and an analysis of the behavior of three strong UV emission lines is presented. It is found that the propensity for various energy relaxation pathways evolves with x as the local environment at the dopant site alters the branching ratios from level to level. It is hoped that the information presented here will stimulate a subsequent investigation that ascertains how the spectra and the energy transfer pathways might vary with dopant site type, point symmetry, and ionic radius as the local environment of the dopant evolves with x.

ACKNOWLEDGMENTS

The authors would like to thank Hongying Peng for her early contributions to this project. The work at Cincinnati was supported in part by the U. S. Army Research Office (Grant No. DAAD19-03-1-0101). The authors acknowledge many technical discussions with J. M. Zavada and the stimulating questions posed by the reviewer.

[1] A. J. Steckl, J. H. Park, and J. M. Zavada, Mater. Today **10**, 20 (2007).
[2] S. Schmitt-Rink, C. M. Varma, and A. F. J. Levi, Phys. Rev. Lett. **66**, 2782 (1991).
[3] K. Takahei, A. Taguchi, H. Nakagome, K. Uwai, and P. S. Whitney, J. Appl. Phys. **66**, 4941 (1989).
[4] U. Hömmerich, E. E. Nyein, D. S. Lee, A. J. Steckl, and J. M. Zavada, Appl. Phys. Lett. **83**, 4556 (2003).
[5] H. Peng, C.-W. Lee, H. O. Everitt, C. Munasinghe, D. C. Lee, and A. J. Steckl, J. Appl. Phys. **102**, 073520 (2007).
[6] J. Neugebauer and C. G. Van de Walle, Appl. Phys. Lett. **69**, 503 (1996).
[7] S. Petit, R. Jones, M. J. Shaw, P. R. Briddon, B. Hourahine, and T. Frauenheim, Phys. Rev. B **72**, 073205 (2005).
[8] J.-S. Filhol, R. Jones, M. J. Shaw, and P. R. Briddon, Appl. Phys. Lett. **84**, 2841 (2004).
[9] D. S. Lee and A. J. Steckl, Appl. Phys. Lett. **83**, 2094 (2003).
[10] J. B. Gruber, U. Vetter, H. Hofsäss, B. Zandi, and M. F. Reid, Phys. Rev. B **70**, 245108 (2004).
[11] The 85 K band edges are measured at the inflection points. The bandgap for AlN is 6.11 eV at 10 K, according to J. Li, K. B. Nam, M. L. Nakarmi, J. Y. Lin, H. X. Jiang, P. Carrier, and S.-H. Wei, Appl. Phys. Lett. **83**, 5163 (2003).
[12] For $x=0.81$, the PLE curves indicate that $^1I_6$ (396 nm) and $^1D_2$ (371 nm) may be weakly excited directly—via $^3P_1$ and $^3P_2$, respectively. For $x=0.39$, Fig. 1 indicates that the $^1I_6 \rightarrow {}^3H_6$ transition overlaps the shallow impurity band, and the PLE of Fig. 3 suggests the possibility of a cooperative effect between indirect and direct excitation mechanisms for some transitions.
[13] This feature was not observed for larger x perhaps because it occurs beyond the accessible spectral range.
[14] Ü. Özgür, H. O. Everitt, L. He, and H. Morkoç, Appl. Phys. Lett. **82**, 4080 (2003).